FULL PAPER

Keyword

steel
research
international

www.steel-research.de

Effect of the Fluid-Dynamic Structure on the Mixing Time of a Ladle Furnace

Renato González-Bernal, Gildardo Solorio-Diaz, Angel Ramos-Banderas,* Enrique Torres-Alonso, Constantin A. Hernández-Bocanegra, and Roberto Zenit

This work shows the analysis of the fluid-structure over the mixing time in a ladle furnace. A 1/7 scale acrylic model is constructed from a 135 t ladle, the injection configuration, and the gas flow injected at the bottom of the model are varied. The techniques applied for this study are Colorimetry, Conductimetry (KCl), and Particle Image Velocimetry (PIV). The results indicate that the number, size, and location of the recirculations in the bulk of the fluid have a noteworthy effect on the mixing time of the ladle. The results show that, for configurations involving one gas injection, the increase in gas flow rate does not diminish the degree of homogenization in the analyzed ladle, which is contrary to the logic regarding the energy state of the system. This is explained by taking into account the fluid dynamics structure obtained for the corresponding cases of study.

1. Introduction

The stirring of liquid steel in the ladle with Argon is a practice universally adopted since the 1960's and was developed to optimize steelmaking processes. It is quite clear that the understanding of the fluid dynamics and the interaction between the involved phases during this operation affects directly the productivity and quality of steel. Agitation of the steel by the injection of gas by porous plugs located at the bottom of the ladle is nowadays a practice used throughout the world, and is commonly referred to as secondary refining. The advantages of this operation in the steelmaking process, when is properly performed, are: reduction of the

processing time, chemical and thermal homogenization of the metal bath, as well as improving the removal of non-metallic inclusions. The great turbulence generated by the rise of bubbles is responsible for improving the kinetics of the reactions, besides the opening that generates on the slag layer is used to feed the ferroalloys. One of the drawbacks of this practice is that, if the proper injection time is not known at high flow rates, there is the possibility of creating an overexposure of the liquid steel to the oxygen and nitrogen of the environment, generating an adverse effect on the steel cleanness. Taking into account the above considerations, it has been suggested to monitor the total oxygen in the steel along agitation time to establish a time where the re-oxidation is minimal and the removal of inclusions is the maximum.[1] It has been proven that the mixing time variable is the parameter that indicates the process efficiency and it has been widely used to represent the state of agitation of a fluid inside a reactor.[2–4] Also, it has been pointed out[5] that the mixing time is influenced by two transport mechanisms: (i) convective flow, that is, macroscopic recirculations generated by the upward gas plume and (ii) turbulent diffusion, which is due to dissipation of the turbulent kinetic energy of the system. It is important to note that at least seven empirical correlations are reported in the literature, depending on the dimensions of the ladle (H, D) and gas flow (Q).[2] Currently, there is great controversy about the effect that can provide the location of the tracer release, as well as the location of the monitoring points on the mixing time. Some experimental works[6–12] reported that dead zones delay the mixing time, however, in other studies[13,14] it has been reported that, under certain operating conditions, there is a single mixing time for each reactor regardless of where the release and monitoring of the tracer is performed when a degree of homogeneity of up to 99.5% is applied. It has also been reported[15–20] that the use of a slag layer always delays the mixing time and its effect can be increased, as the thickness and viscosity of the slag is raised. This phenomenon has been explained[2] and is attributed to the energy loss of the injected gas to the system. However, it has also been reported[12] that low density slags, related with very low argon flow conditions, can have an opposite effect on the mixing time, which has not been explained from the hydrodynamic viewpoint. It is important to note that in the vast majority of studies performed, the effect of the argon flow is inversely correlated with the mixing time, which to some extent has a logic, since the higher gas flow the higher the rate of specific energy input to the system. Though, it is

Prof. A. Ramos-Banderas, Prof. E. Torres-Alonso,
Prof. C. A. Hernández-Bocanegra
Graduate Program in Metallurgy, Morelia Technological Institute, C.P. 58120 Morelia Mich., México
E-mail: arblss@hotmail.com

R. González-Bernal
Graduate Student, Thermofluids-UMSNH, Address: Av. F. J. Mujica S/N, C.P. 58140 Morelia Mich., México

Prof. G. Solorio-Diaz
Thermofluids-Mechanical Engineering UMSNH, F. J. Mujica S/N, C.P. 58140, Morelia Mich., México

Prof. C. A. Hernández-Bocanegra
CATEDRAS-CONACyT, Benito Juarez, CDMX 03940, México

Prof. R. Zenit
Materials Research Institute – UNAM, Cd. Universitaria, Coyoacán, CDMX 04510, México

**ADVANCED
SCIENCE NEWS**

www.advancedsciencenews.com

**steel
research**
international

www.steel-research.de

very clear that the fluid-dynamic structure inside the ladle is the main factor affecting the mixing time.[6,7,10,21–23] In this work, a model of acrylic at reduced scale of a ladle of 135 t was made, and the configuration of the injection and the flow of gas were varied. The techniques applied for this study were Colorimetry, Conductimetry (KCl), and Particle Image Velocimetry (PIV). The aim of this work was to determine the effect of the fluid-dynamic structure on the mixing time of a ladle.

2. Experimental Section

2.1. Construction of the Physical Model

A physical model was developed, scaled at 1/7 of the prototype used in the industry, which was constructed in transparent acrylic of 4.5 mm thickness. **Figure 1**a shows the model dimensions, position of the gas inlets, as well as the location of the two conductivity probes used to determine the mixing time. Taking as a

starting point the flow data of Ar used in the plant, the dynamic scaling was carried out using the modified Froude number (Fr) that relates the inertial to the flotation forces. For this purpose, it was employed the set of Equations 1–4.

$$Fr = \frac{\rho_g \cdot u^2}{\left(\rho_l - \rho_g\right) \cdot g \cdot l} \tag{1}$$

$$u = \frac{4 \cdot Q}{\pi \cdot d^2 \cdot N} \tag{2}$$

Substituting Equation 2 into 1 yields:

$$Fr_m = Fr_p = \frac{1.621 \cdot \rho_g \cdot Q^2}{\rho_l \cdot d^4 \cdot N^2 \cdot g \cdot H} \tag{3}$$
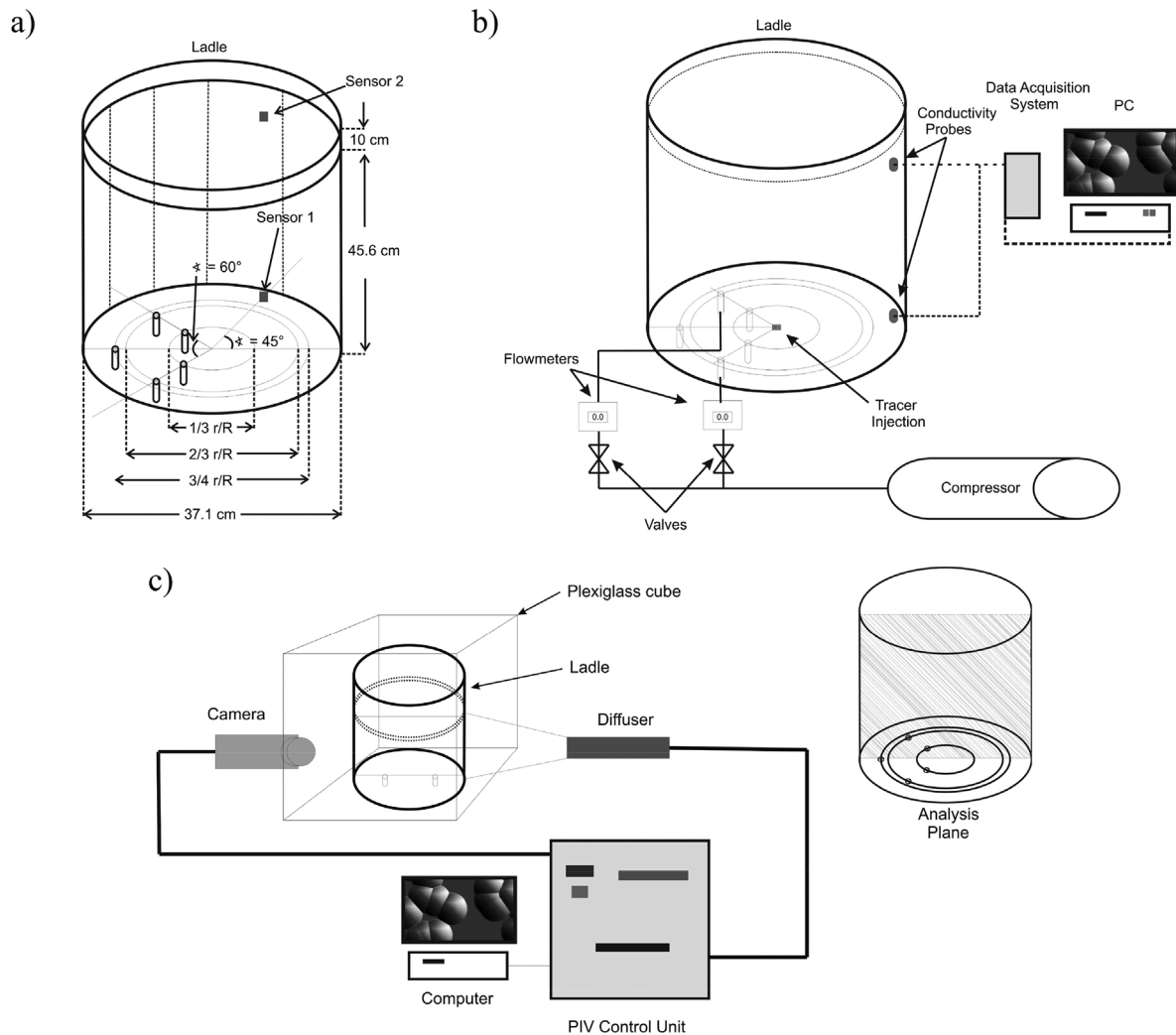

Figure 1. Ladle Geometry of the 1/7 scaled model, a) ladle dimensions, b) experimental setup for mixing time measurements, and c) experimental setup for PIV and analyzed plane location.

Assuming that the model has the same number of tuyeres as the prototype, Equation 4 was used to determine the gas flow in the model.
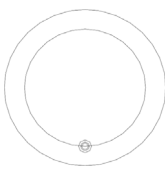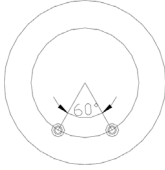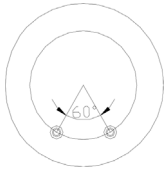
$$\left(\frac{Q_m}{Q_p}\right)^2 = \left(\frac{\rho_{g,p}}{\rho_{g,m}}\right) \cdot \left(\frac{\rho_{l,m}}{\rho_{l,p}}\right) \cdot \left(\frac{d_m}{d_p}\right)^4 \cdot \left(\frac{H_m}{H_p}\right) \tag{4}$$

where u is the velocity; Q, is the gas flow; ρ_l and ρ_g are the liquid and gas density, respectively; g, is the gravity force; l, is the characteristic length that can be replaced by the bath height (H); N, is the number of tuyeres; d, is the inner diameter of the tuyere; and the subscripts m and p, refer to model and prototype, respectively. The maximum gas flow used in the industry to perform the chemical adjustment and desulfurization is 1500 Nm^3 min^{-1}, a gas flow of 923.2 Nm^3 min^{-1} was also used to determinate the effect of this variable on the mixing time and, in turn, to minimize the slag layer opening. Another variable that was taken into account was the configuration of the gas injection. The cases of study, which combine gas flow and injection positions, are presented in **Table 1**, totaling six cases: three injection arrangements and two gas flows. For the two injection arrays, each uses half of the calculated total gas flow.

2.2. Techniques of Colorimetry, Tracer Injection, and Measurement of Mixing Time

The colorimetry technique consists of injecting a visible tracer substance that does not interfere with or modify the fluid dynamics of the system.[6,22,24] In this work, 20 ml of vegetal Red 40 colorant was employed as visible tracer dispersion in the model, this substance does not affect the conductivity and density of the water. In this way, it is possible to visualize the path of the water displacement to identify zones of recirculation of

Table 1. Arrangements of the ladle.

Case	Number of tuyeres	Scheme	Gas flow rate per tuyere	Location of tuyere
1A	1		a) 4.90 NL min^{-1}	¾R
1B			b) 3.00 NL min^{-1}	
2A	2		a) 2.45 NL min^{-1}	2/3R y 60° of separation between the tuyeres
2B			b) 1.50 NL min^{-1}	
3A	2		a) 2.45 NL min^{-1}	1/3R y 60° of separation between the tuyeres
3B			b) 1.50 NL min^{-1}	

low speed or limited mixing. The mixing time is defined as the time in which the changes in ion concentration have a deviation of less than ±5% at steady state in a liquid bath. This definition refers to the criterion of the time in which it takes to homogenize to 95% the liquid bath maintained in constant movement, which is in a container.[25] The mentioned above belongs to the stimulus-response techniques. In this work, a stimulatory agent (KCl with a molar concentration of 3.35 M) dissolved in water was used as a tracer solution. The experimental system is shown in Figure 1b.

First, the gas (air) was injected through the bottom of the ladle until a quasi-steady state flow pattern was reached, the tracer solution was fed in the center of the ladle model through the bottom using a transparent hose of 0.0032 m diameter which was controlled by a pipette. The ferroalloys in the industry are fed taking advantage of the slag layer aperture and incorporated to the main flow of the fluid-dynamic structure. Hence, in this work the selected location permitted the tracer to reach the main flow, which previously observed via colorimetry technique.

For this purpose, the hydrostatic pressure gradient was used, favoring that the tracer drag was carried out by the kinematics of the water. Conductivity measurements were performed in the positions indicated in Figure 1b; the upper probe was immersed 0.1 m into the water at 0.05 m from the sidewall, the lower probe was at 0.1 m from the bottom, and 0.0 m from the sidewall since, at being away from the area where the plume is formed, the level of turbulence is lower and the readings are more stable. Conductivity probes Oakton 3/4NPT (series WD-35820-20) with graphite electrode and cell constant $K = 1$ were used. The signal was acquired and controlled by an Oakton Conductivity Meter (1000 Series) every second until the experiment was completed (140 s on average). This data was sent to a Data Acquisition System (Keithley model KNM-TC42-RS232-C) and this, in turn, to a computer, as illustrated in Figure 1b. The conductivity values were changed to concentration values by a calibration curve and its respective adjustment to a third degree polynomial Equation. To obtain the mixing curves, the average data corresponding to five experiments per case was used.

2.3. Particle Image Velocimetry Technique (PIV)

To obtain the velocity fields and pathlines in the scale model, a PIV technique was employed, major details of this technique has been previously described.[26,27] A scheme of the PIV equipment (Dantec Systems®) used in this work is shown in Figure 1c, this equipment has a green laser Nd: YAG of double pulse with wavelength of 532 nm. To obtain pulses of light energy, the laser signal is interrupted and thus emits pulses of 250 µs, which is the duration of the excitation of the lamp in the laser cavity. The energy output of the laser is 20 mJ, but can be increased to a value of 500 mJ of pulsed radiation with an optical transmission greater than 90%. The light sheet forming the laser was positioned in the plane indicated in Figure 1c by means of a positioner with three-dimensional movement controlled by the computer. To achieve perpendicular photographs to the plane of analysis, a cube of transparent acrylic of 0.006 m thickness was constructed, leaving at least 0.03 m of distance between the cube and the external wall of the ladle model. This space was filled

ADVANCED
SCIENCE NEWS

www.advancedsciencenews.com

steel
research
international

www.steel-research.de

with water, which was previously treated with a vacuum pump to eliminate the presence of bubbles. Polyamide particles of 20 μm, with a density of 1030 kg m^{-3}, were incorporated into the fluid before initializing the system. A cross-linking procedure, using Fourier transforms, was used to process the recorded signals; and a Gaussian distribution function was used to locate the maximum peak displacement with an accuracy of the order of sub-pixels. The signals were recorded by a Dantec Systems® charge chamber device (CCD), which uses 90 mm Nikon lenses, and then processed using the commercial Flow Map® software, obtaining the velocity vector fields. Four quadrants were used for each plane using analysis areas 225 × 225 mm, which in turn were subdivided generating a mesh of 62 × 62 mm per sub-frame, achieving a density of vectors of 3844 per quadrant. The four quadrants were overlapped by adding a density of vectors of 15 376 that make up each of the planes presented. On average, 250 images were acquired in 2 min per quadrant, 1000 in total for each plane. Finally, the images of the vector fields are the result of the averaged images. Also, with the processing of the obtained data it was possible to obtain the flow lines.

3. Results and Analysis

Figure 2 shows colorant dispersion images for the studied cases at times of 4, 6, 8, 10, and 16 s, which was added to the water once the quasi-steady state was reached. For cases 1A and 1B, a very similar fluid flow behavior was observed with a large recirculation that moves the entire volume of fluid clockwise (Point 1 of Figure 2c and c'), also, it can be seen how the advance of colorant in the case 1A is slower than for case 1B, even though the latter had lower gas flow rate. For both cases, the injected colorant, in the $r/R = 0$ position at the bottom of the ladle, was dragged by the movement of the fluid to the side wall, but a very different behavior was observed during its ascent toward the bath surface: for case 1A, the colorant begins to disperse approximately to half the height of the ladle (Figure 4b), for case 1B, the dispersion occurs immediately upon impacting the sidewall of the ladle (Figure 2a'). From this observation, it could be deduced a reduction in the mixing time of the fluid contained in the ladle for case 1B. There is undoubtedly a conjugation of the fluid-dynamic phenomena that directly affect the mixing time, since it can be observed that the main recirculation convectively drags the colorant toward the surface of the ladle, avoiding that this is dispersed toward the center of the same. However, for case 1B, the volume of fluid that circulates through the bottom impacts the sidewall at a lower point than for case 1A, thereby increasing the turbulent diffusion component, favoring a great dispersion of the colorant toward the center of the recirculation.

To explain the above, we proceeded to analyze the velocity fields and the flow lines obtained by PIV for these two cases, which are illustrated in **Figure 3**. These images perfectly define the size, position, and orientation of the eye of the main recirculation that is presented for both cases. These recirculations take an ellipsoidal shape in their central part, but in the case 1A, it is wider on its smaller axis and shorter on its major axis compared to that of case 1B. Another significant difference is the inclination of these ellipses, while for case 1A the eye of the recirculation has a slope of approximately 22 degrees

counterclockwise with respect to the horizontal, for case 1B a steeper slope of approximately 30 degrees is presented in the same direction, as illustrated in Figure 3b and d. This inclination of the main recirculation is responsible for directing the fluid and impacting at a lower point of the sidewall for the case 1B. Therefore, it is possible to observe an increase in the flow velocity (point 2 of Figure 3a,c) given the reduction of area that is generated between the recirculated volume and the bottom wall, which is explained as a function of the wall-type effect of the recirculation, which prevents diffusion and homogenization of the colorant. With this analysis, the importance of the fluid-dynamic structure over the mixing time and the way in which the energy is distributed in the bath was verified, even beyond the increase of energy provided by the major gas flow rate.

By analyzing cases 2A and 2B, it is observed that the advance of the colorant dispersion in the ascent zone is very similar between these cases, with a minimum delay for case 2B, as illustrated in Figure 2f', thus forming a zone at the center of the plane of low-dispersion or very low-motion that it is easily identified by the absence of colorant (Figure 2g'). Comparing the advance of colorant in the area of ascent of these two cases against the two cases discussed before at the beginning of the colorant supply, a greater speed of advance is observed. This result is related to the flow structure, as can be seen in **Figure 4** for cases 2A and 2B, respectively. In these cases, a large recirculation is presented at the center of the analysis plane, with a spiral shape in both cases, which is more distorted for case 2B. In addition, a smaller secondary recirculation is located in the lower right corner for both cases. This is responsible for deflecting and deforming the main recirculating flow, as illustrated in Figure 4b and d. This diverted flow, fed from the upper right side, hits the bottom of the ladle harder in case 2A, while for case 2B the secondary recirculation manages to divert the main flow more effectively, since it is larger than in case 2A. Due to that, a decreasing velocity component on the y-negative axis is observed, causing a change of slope in the descending flow lines as shown in Figure 4b and d. After the impact of the descendant flow with the bottom of the ladle, an increase in speed is observed as illustrated by point 3 of Figure 4a and c. However, despite of the flow impacted with the bottom tends to rise, the damping effect of the low speed zone of the main recirculation aligns again the flow with the bottom wall, and the velocity of the flow decreases as it approaches to the lower left corner of the plane (point 4 of Figure 4a,c). This explains why, for these two cases, the advance of the released colorant approaches the left wall and rises very close to it, in a similar way to the first two cases analyzed.

Figure 5 shows the fluid-dynamics structure obtained for cases 3A and 3B. It is observed that the dispersion of colorant is very different than the four cases previously analyzed, the colorant no longer advances through the bottom of the ladle to rise next to the sidewall; the colorant advances a little through the bottom and rises immediately without approaching the sidewall. This phenomenon is more noticeable for case 3B. As observed in the dye dispersion images of Figure 2k and k', two large recirculations are presented for these two cases, which are associated with areas of low velocity or areas where colorant diffusion is very slow. To perform a more in-depth analysis, the results obtained by the PIV were studied, which are shown in
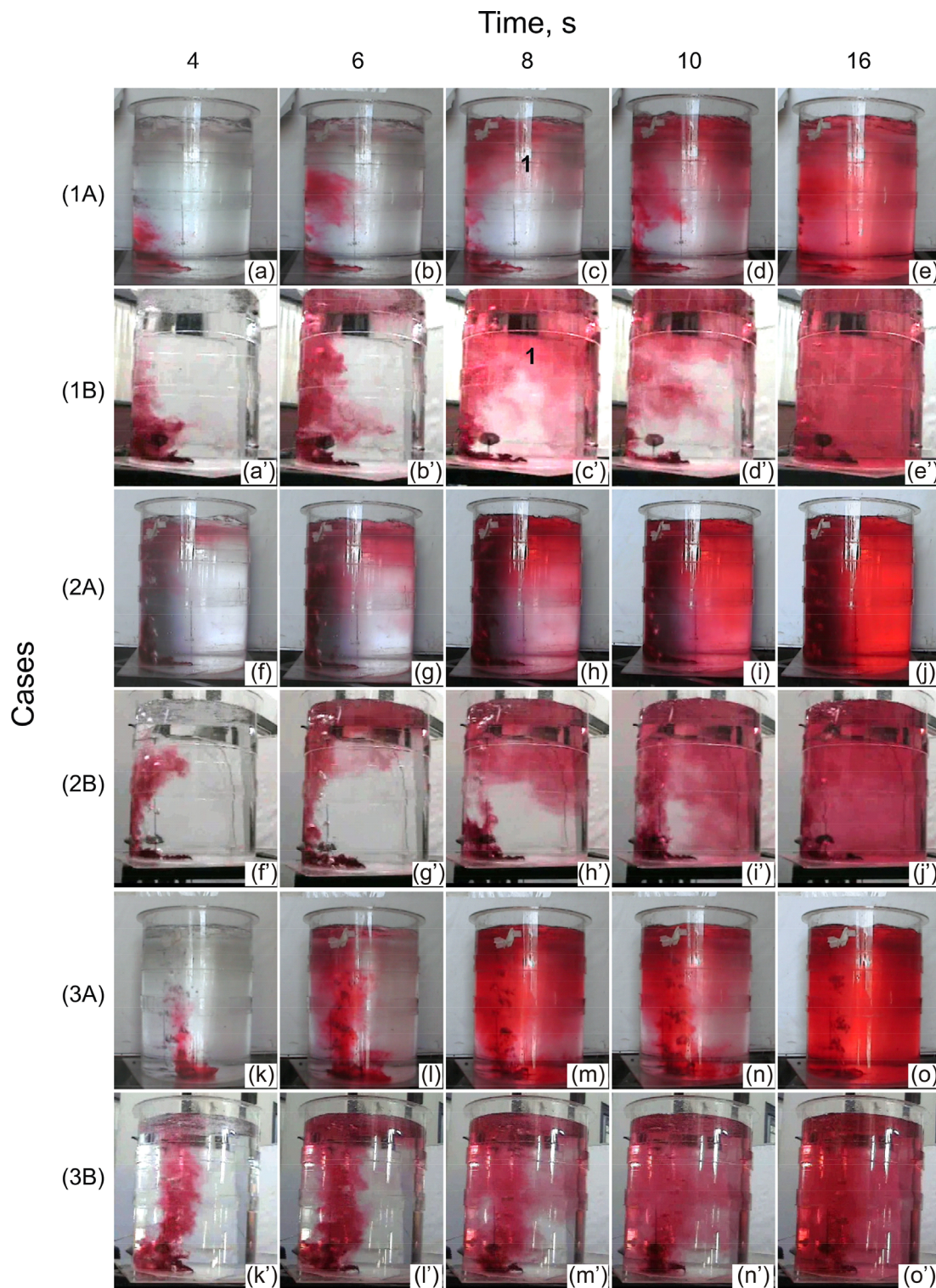
ADVANCED
SCIENCE NEWS
www.advancedsciencenews.com

steel
research
international
www.steel-research.de

Figure 2. Colorant-dispersion photographs at different times after injection.

Figure 5. With the images of the velocity fields, it could be corroborated in a very precise way the observed in the images of the colorant dispersion, that is, the areas where the dispersion of the colorant is delayed correspond exactly to the areas where the flow recirculates at very low velocity, which are identified by points 5 and 6 of Figure 5a and c. The images of the streamlines of Figure 5b and d helped to determinate the precise size and shape of the fluid-dynamic structure; it can be seen that the
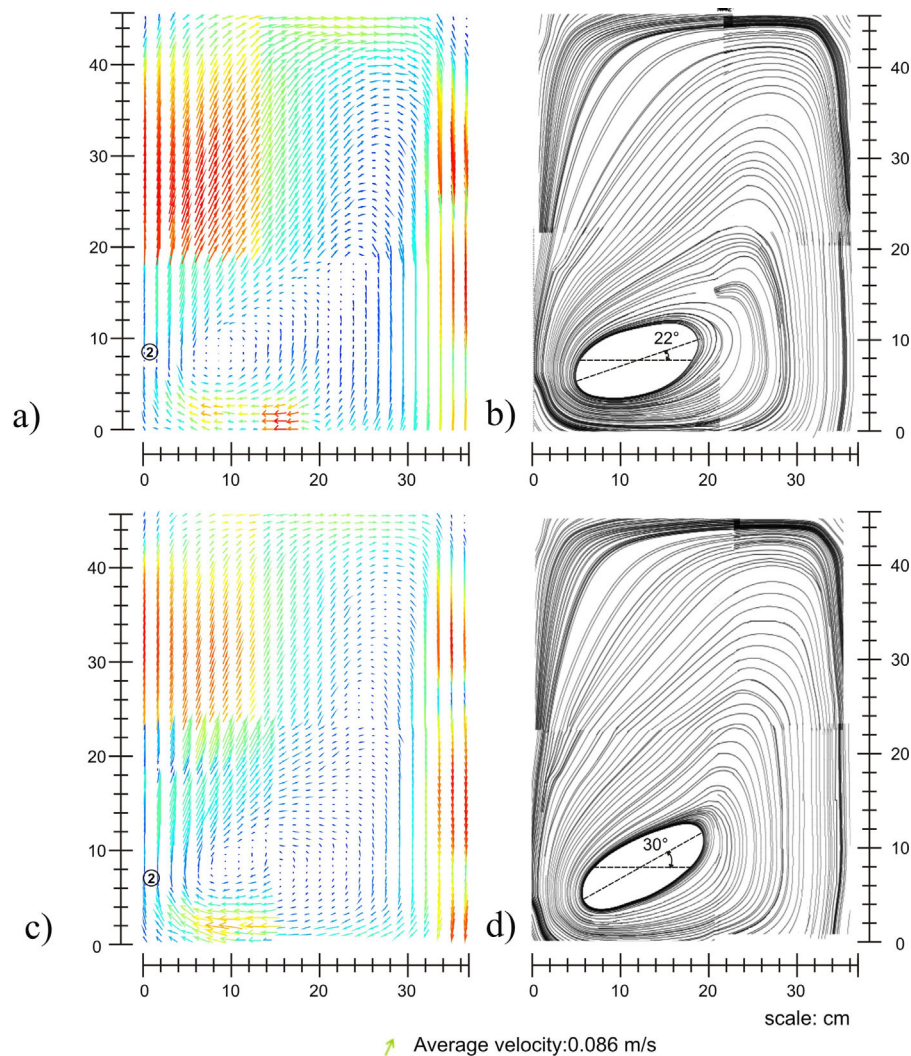
Figure 3. Average velocity fields and streamlines obtained by PIV. a and b) Cases 1A, c and d) cases 1B.

location of the recirculations is approximately the same for both cases. Figure 5d indicates that the left recirculation (point 5) for case 3B is longer, compared to its homologous in case 3A, coming even closer to the bottom of the ladle. This difference helped to explain the fastest rise of the colorant in this case compared to case 3A, since this recirculation has a wall-type effect which prevents the fluid from reaching the sidewall of the ladle. The obstacle represented by this large recirculation, defines in a shorter time the upward trajectory of the colorant for case 3B. The second recirculation shown in both cases (3A, 3B) in Figure 5b and d (point 6) is located in the upper right side, presenting an oval shape, and whose upper limit is too close to the bath surface. It is easier to visualize in Figure 5b and d that the size, the shape, and location of this recirculation are similar in both cases, promoting low velocity zones at their interior, as it is illustrated in points 3 and 4 of Figure 5a and c.

After the analysis of the fluid-dynamic structure by PIV and its corresponding tracer dispersion, the mixing times at 95% were evaluated with the previously described technique. **Figure 6** shows the dimensionless average of the signals measured by the probes for case 1A. It can be observed that the signal of the probe located at the top is the first to register the signal, and it is until ≈93 s that the two signals reach similar values, this result obeys the fluid-dynamic structure since the great recirculation drags the tracer by passing first through the upper probe. The fluctuation of the data observed in the curves is typical of experimental measurements and is most noticeable in the upper probe due to the turbulence levels provided by the gas plume, which is indicated by the disordered tracer dispersion as the fluid advances. The summary of mixing times is presented in **Figure 7** for the different cases addressed in this study. As can be seen, cases 1A and 1B are the ones with the shortest mixing times and cases 3A and 3B are the ones that are the slowest to achieve homogenization. With the configuration of the cases (1A and 1B) with argon injections more distant from the center of the ladle, the results of mixing time found are in agreement with the results previously reported.[6,10,21,28,29] They attributed the reduction of the mixing time to one of the hypotheses proposed by Szekely,[5] claiming that if the injection tuyere approaches the sidewall of the ladle, small eddies are formed which are
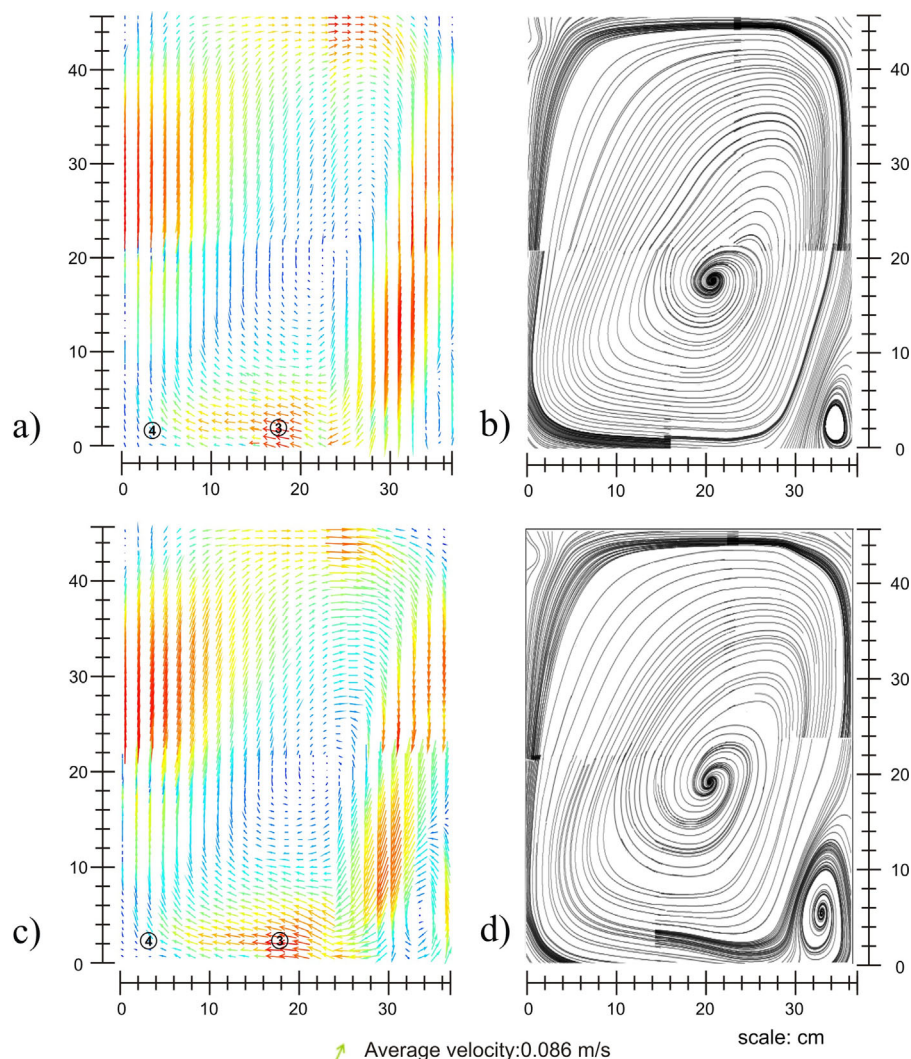
ADVANCED
SCIENCE NEWS
www.advancedsciencenews.com

steel
research
international
www.steel-research.de

Figure 4. Average velocity fields and streamlines obtained by PIV. a and b) Cases 2A, c and d) cases 2B.

responsible for mixing. However, the explanation proposed in this work is very different, in the present work it was determined that the mixing phenomenon is strongly affected by the number, size, shape, and location of the recirculations, as suggested.[13] It is also worthy to mention than results of mixing time for case 1B were compared with the obtained via mathematical simulation for the authors[23] and they matched acceptably well.

It is known that, in general, the results of the mixing depend on factors such as molecular diffusion, convective flow, and turbulent diffusion. In this case, it has been determined that the convective flow has a noteworthy effect when it comes to chemically homogenizing the metal bath. Starting from this, it can be stated that due to two large recirculations that exhibit the cases 3A and 3B, it is logical that their mixing times are the highest in relation to the other cases, since cases 1A and 1B only have one large recirculation, and although cases 2A and 2B have two recirculations, one of them is too small.

From this observation, it is easy to establish that the difference between cases 2A and 2B is that in the latter, the smallest

recirculation is larger than its homologous case 2A and hence the increase in the mixing time. Something similar occurs between cases 3A and 3B since precisely one of the recirculations of case 3B is larger than its counterpart in case 3A, which causes its mixing time to increase.

From the results obtained for the mixing time, it can be determinate that the energy state of the system is fundamental to predict the homogenization of the bath, but no less important is the study of the fluid-dynamic structure that could be obtained from the different arrangements of plugs commonly found in the industry. Therefore, studying the quantity, size, shape, and distribution of the recirculations helps to understand and optimize the chemical and thermal homogenization of these types of systems. Thus, before making any decision regarding this issue in the plant, it is necessary to make a rigorous analysis of the fluid-dynamic structure that could affect both the quality and the productivity of the process. Because, until now it is believed that the decrease of mixing time is directly proportional to the increase in gas flow, which does not always occur as demonstrated in cases 1A and 1B. Finally, it is important to
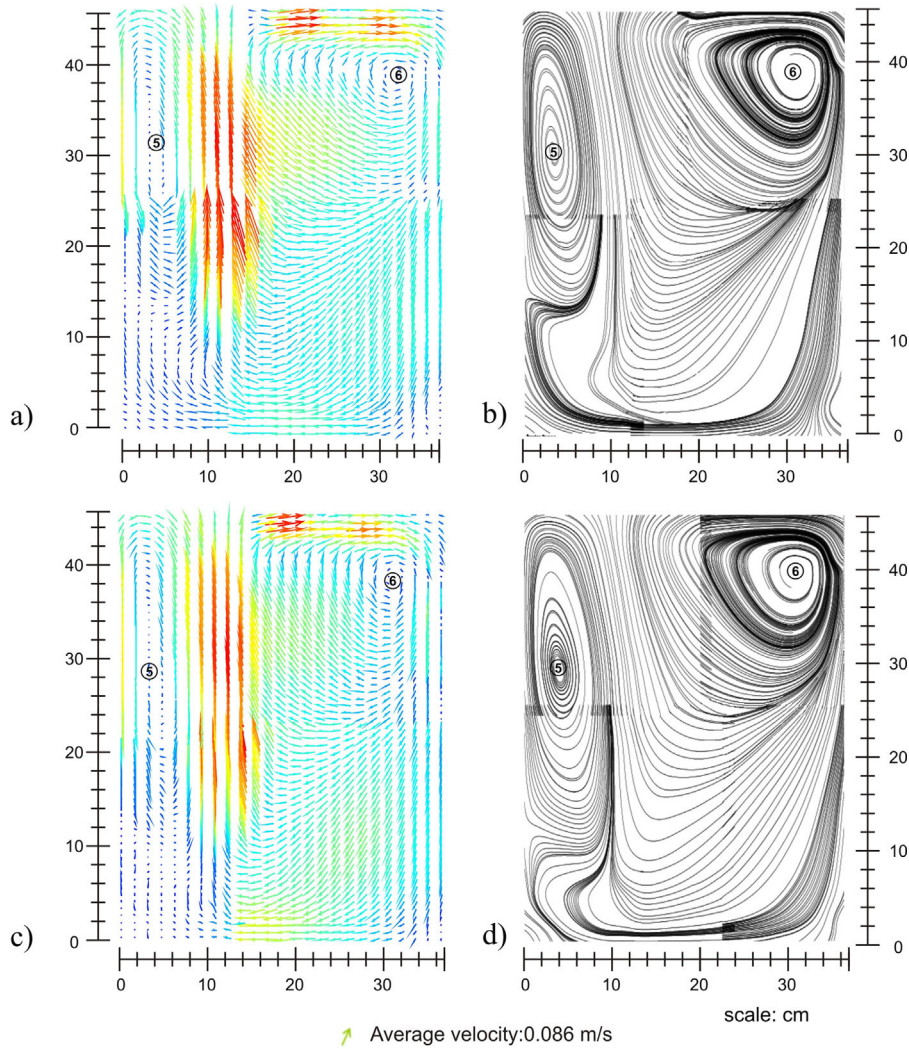
**ADVANCED
SCIENCE NEWS**

www.advancedsciencenews.com

**steel
research**
international

www.steel-research.de

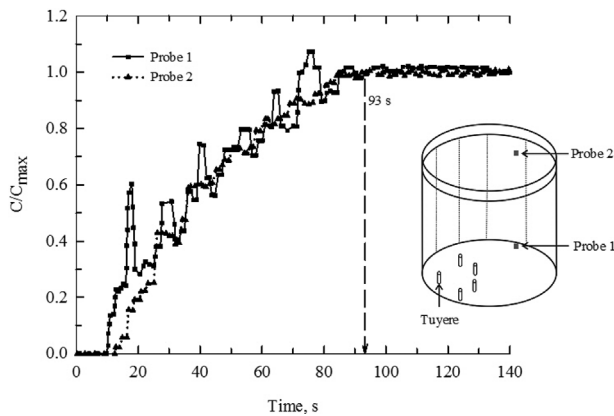**Figure 5.** Average velocity fields and streamlines obtained by PIV. a and b) Cases 3A, c and d) cases 3B.

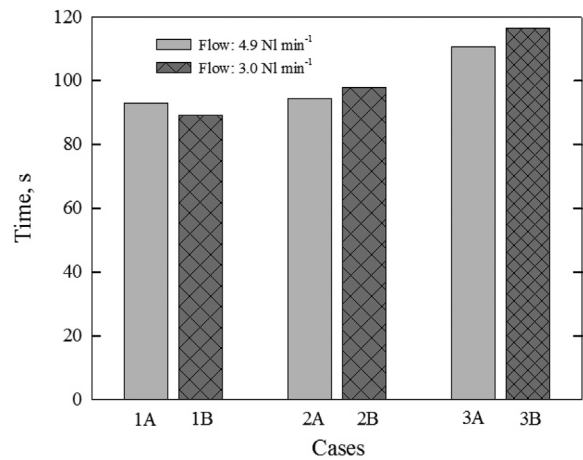**Figure 6.** Experimental curves of dimensionless concentration versus time, for case 1A.

Figure 7. Mixing time results for all cases.

**ADVANCED
SCIENCE NEWS**
www.advancedsciencenews.com

**steel
research**
international

www.steel-research.de

mention that given the actual process conditions the use of physical modeling to study the fluid dynamics structure becomes very relevant.

4. Conclusions

In this work, an analysis of the fluid-dynamic structure has been carried out using colorant dispersion, tracer injection and PIV techniques for three different positions of the gas injection. Two different gas flow rates were also studied in a scaled physical model of a steel ladle furnace. The main conclusions of this work are given below.

1) Colorant and tracer dispersion techniques were complemented fairly well with PIV results, easily identifying areas of stagnation or recirculation within the ladle model.

2) It has been determined that the mixing times depend largely on the fluid-dynamic structure, that is, the quantity, shape, distribution, and size of the recirculations formed inside the ladle. It was found that cases 3A and 3B have the highest mixing times and, on the contrary, cases 1A and 1B present a chemical homogenization in shorter times. On the other hand, it is not necessary to increase the gas flow rate to reduce the mixing time, as was determined for the cases 1A and 1B in which the opposite happened, in addition, an excess of argon gas flow could have adverse consequences to the process such as re-oxidation or a reduction in the life of the refractory of the ladle.

3) It was found that at a lower gas flow rate (case 1B), the mixing times were lower because the turbulent dispersion in this case was increased due to the great tilt of the main recirculation.

Conflict of Interest

The authors declare no conflict of interest.

[1] C. G. Mendez, N. Nigro, A. Cardona, S. S. Begnis, W. P. Chiapparoli, *Physical and Numerical Modelling of a Gas Stirred Ladle, MECOM 2002*, Santa Fe-Paraná, Argentina **2002**, *XXI*, 2646.

[2] D. Mazumdar, R. I. L. Guthrie, *ISIJ Int.* **1995**, *35*, 20.

[3] T. Haiyan, G. Xiaochen, W. Guanghui, W. Yong, *ISIJ Int.* **2016**, *56*, 2161.

[4] D. Mazumdar, P. Dhandapani, R. Sarvanakumar, *ISIJ Int.* **2017**, *57*, 286.

[5] J. Szekely, G. Carlsson, L. Helle, *Ladle Metallurgy*, Springer-Verlag, New York Inc. **1989**, p. 52.

[6] J. Mietz, F. Oeters, *Steel Res. Int.* **1988**, *59*, 52.

[7] J. Mietz, F. Oeters, *Steel Res. Int.* **1989**, *60*, 387.

[8] D. Mazumdar, R. I. L. Guthrie, *Metall. Mater. Trans. B* **1986**, *17B*, 725.

[9] U. P. Sinha, M. J. McNallan, *Metall. Mater. Trans. B* **1985**, *16B*, 850.

[10] S. Joo, R. I. L. Guthrie, *Metall. Mater. Trans. B* **1992**, *23B*, 765.

[11] J. Aoki, B. G. Thomas, J. Peter, K. D. Peaslee, *Experimental and Theoretical Investigation of Mixing in a Bottom Gas-Stirred Ladle*, AISTech 2004, Nashville, TN **2004**, p. 1045.

[12] A. N. Conejo, S. Kitamura, N. Maruoka, S. J. Kim, *Metall. Mater. Trans. B* **2013**, *44B*, 914.

[13] G. G. Krishnamurthy, S. P. Mehrotra, A. Ghosh, *Metall. Mater. Trans. B* **1988**, *19B*, 839.

[14] G. G. Krishnamurthy, S. P. Mehrotra, A. Ghosh, *Proc. of the 6th Process Technology Conf., 5th Int. Iron & Steel Congress*, Washington, D.C. **1986**, p. 401.

[15] S.-H. Kim, R. J. Fruehan, *Metall. Mater. Trans. B* **1987**, *18B*, 381.

[16] H. Liu, Z. Qi, M. Xu, *Steel Res. Int.* **2011**, *82*, 440.

[17] S. Yamashita, K.-I. Miyamoto, M. Iguchi, M. Zeze, *ISIJ Int.* **2003**, *43*, 1858.

[18] D. Mazumdar, D. S. Kumar, *Mixing Times and Correlation for Dual Plug Stirred Ladle: Quantifying the Role of an Upper Buoyant Phase*, Oxygen Steelmaking (Metsoc. CIM), Hamilton, Canada **2004**, p. 311.

[19] S. P. Patil, D. Satish, M. Peranandhanathan, D. Mazumdar, *ISIJ Int.* **2010**, *50*, 1117.

[20] J. W. Han, S. H. Heo, D. H. Kam, B. D. You, J. J. Pak, H. S. Song, *ISIJ Int.* **2001**, *41*, 1165.

[21] M.-Y. Zhu, T. Inomoto, I. Sawada, T.-C. Hsiao, *ISIJ Int.* **1995**, *33*, 472.

[22] J.-U. Becker, F. Oeters, *Steel Res. Int.* **1998**, *69*, 8.

[23] C. A. Llanos, S. Garcia, J. A. Ramos-Banderas, J. de J. Barreto, G. Solorio, *ISIJ Int.* **2010**, *50*, 396.

[24] J. C. U. Avila, G. Solorio-Diaz, J. A. Ramos-Banderas, H. Vergara H., H. C. Gutiérrez, *Optimización del Tiempo de Mezclado en una Olla de Colada Continua*, Memorias del XVI Congreso Internacional Anual de la SOMIM, Nvo. León, México **2010**, p. 205. http://somim.org.mx/articulos2010/memorias/memorias2010/A5/A5_234.pdf

[25] S. Ni, H. Wang, J. Zhang, L. Lin, S. Chu, *Acta Metall. Sin. (Engl. Lett.)* **2014**, *27*, 1008.

[26] R. P. Nunes, J. A. M. Pereira, A. C. F. Vilela, F. T. V Der Laan, *JESTEC* **2007**, *2*, 139.

[27] R. P. Nunes, F. T. Van Der Laan, INFOCOMP *J. Comput. Sci.* **2007**, *6*, 56.

[28] G. Akdogan, R. H. Eric, *Metall. Mater. Trans. B* **1999**, *30B*, 231.

[29] S. Asai, T. Okamoto, J.-C. He, I. Muchi, *Trans. Iron Steel Inst. Jpn.* **1983**, *23*, 43.